www.ietdl.org

Published in IET Renewable Power Generation
Received on 30th March 2010
Revised on 12th October 2010
doi: 10.1049/iet-rpg.2010.0052

ISSN 1752-1416

Smart energy management system for optimal microgrid economic operation

C. Chen S. Duan T. Cai B. Liu G. Hu

Power Electronics Research Center, College of Electrical and Electronic Engineering, Huazhong University of Science and Technology, Wuhan 430074, People's Republic of China
E-mail: ccsfm@163.com

Abstract: This study presents a smart energy management system (SEMS) to optimise the operation of the microgrid. The SEMS consists of power forecasting module, energy storage system (ESS) management module and optimisation module. The characteristic of the photovoltaics (PV) output in different weather conditions has been studied and then a 1-day-ahead power forecasting module is presented. As energy storage needs to be optimised across multiple-time steps, considering the influence of energy price structures, their economics are particularly complex. Therefore the ESS module is applied to determine the optimal operation strategies. Accordingly, multiple-time set points of the storage device, and economic performance of ESS are also evaluated. Smart management of ESS, economic load dispatch and operation optimisation of distributed generation (DG) are simplified into a single-object optimisation problem in the SEMS. Finally, a matrix real-coded genetic algorithm (MRC-GA) optimisation module is described to achieve a practical method for load management, including three different operation policies and produces diagrams of the distributed generators and ESS.

1 Introduction

The deregulation in the electric power industry and pressing concerns about global environmental issues as well as the increasing energy consumption have led to an increase in installation capacity of distributed generation (DG) sources and energy storage system (ESS) [1–4]. These sources comprise several technologies, such as diesel engines, microturbines, and fuel cells either in combined heat and power operation or purely for electricity production, photovoltaics (PV), small wind turbines, hydroturbine etc. The coordinated operation and control of DG sources together with storage devices such as flywheels, energy capacitors, batteries and controllable loads such as water heaters and air conditioners is central to the concept of microgrids [5, 6]. Microgrids mostly operate interconnected to the utility grid, but also can turn into an islanded mode, in case of external faults. From the grid's point of view, a microgrid can be regarded as a controllable entity within the power system that can be operated as a single aggregated electrical load, giving attractive remuneration, even as a small source of power or ancillary service supporting the network [7].

Recent developments and advances in energy storage and power electronics technologies are making the application of energy storage technologies a potentially viable solution for the microgrid, allowing the system to be operated in a more flexible, economic manner. Sortomme and El-Sharkawi [8] using particle swarm optimisation, reduced the costs of microgrids with controllable loads and battery storage by selling stored energy at high prices and shave peak loads of the larger system. Chakraborty *et al.* [9] used linear programming algorithms to minimise microgrid operation cost and optimise battery charge states. Marnay *et al.* [10] using Berkeley Lab's distributed energy resources customer adoption model, optimised electrical and thermal storage charge scheduling to maximise benefits owing to the energy pricing differences between on-peak and off-peak periods. Dukpa *et al.* [11] propose a new optimal participation strategy for a wind electric generator (WEG) that employs an energy storage device for participating in the day-ahead unit commitment process. Taking stochastic power output into account, the authors have also proposed a novel smart energy management system (SEMS) that can coordinate power forecasting, energy storage and energy exchanging together and then make proper short-term scheduling to minimise the total operation cost. SEMS identifies optimal operating schedules based on available distributed energy resources (DER) equipment options and their associated capital and operating and maintenance (O&M) costs, load forecasting, energy price structures and fuel prices. Instead of conventional solar forecasting, power forecasting module of PV system with 1-day-ahead weather forecasts is presented for the SEMS. Then, a matrix real-coded genetic algorithm (MRC-GA) is applied to minimise the microgrid cost, in which each GA chromosome consists of a two-dimensional real number matrix representing the generation schedule of ESS and DG sources.

The paper is organised as follows. In Section 2, the features of the DG sources are analysed and the stochastic characteristic of the DG power output is pointed out, e.g. wind power or solar power will change with the variation of wind speed and direction, solar irradiation and

circumstance temperature. The neural network (NN) is incorporated to avoid complexities of mathematical model-based statistical prediction in SEMS. Based on the output of the forecasting module, the SEMS optimisation module chooses a predesigned optimisation schemes such that the operation cost can be minimised. The information of the forecasting module is also utilised to define the threshold for charging and discharging rate for a particular hour in advance. In Section 3, MRC-GA is used for the optimisation module. In each optimisation step, the power balance and storage states are considered to obey the physical constraints. The output of this module defines the direction and amount of the power flow between sources, storages, loads and grid in a cost-optimised way. In Section 4, we present and discuss results obtained under the computational simulations. Conclusions are given in Section 5.

2 Smart energy management system

A typical SEMS is shown in Fig. 1. The objective of the SEMS is to generate suitable set points for all the sources and storages in such a way that economically optimised power dispatch will be maintained to fulfil certain load demand. Because wind power or solar power always change with the variation of wind speed and direction, solar irradiation and circumstance temperature, generation forecast as well as some fast online algorithms are used to define the energy availability and, finally, to define the optimised power dispatch signals to the loads. The use of energy storage requires an optimisation scheme that considers the time-integral part of the load flow. Therefore the energy management has to perform energy scheduling a single day or multiple days ahead. An intelligent energy management system is thus required which enables short-term energy allocation scheduling at minimised costs based on power generation and load demand. The SEMS optimises the microgrid operation according to the open market prices, the bids and the forecasted generation of the DG sources, and the forecasted loads, and sends signals to the controllers of the DG sources to be committed, and if applicable, to determine the level of their production.

2.1 Power forecasting module

The prediction of power generation is a complicated task for the microgrids since most DG sources connected are renewable energy sources whose power generation varies largely with the external conditions like sunshine, temperature etc. However, on the other hand, designing an efficient controller needs prediction of the generation with considerable accuracy. Forecasting of renewable generation is a challenging task and its relevance increases rapidly with more penetration of renewable energy sources in the power grid. In the proposed SEMS, a neutral network [12–14] is incorporated to forecast power generation of a PV energy source, and it can be easily extended to the other renewable-based energy sources. Knowledge of available future generation from renewable sources lets the SEMS to store energy in advance, giving the system more flexibility to take advantage of real-time grid pricing by avoiding purchases or making a well-timed sale.

For PV array, there are many factors that can influence the output character such as solar irradiation, array transfer efficiency, installation angle, atmospheric pressure, temperature and so on [15–17]. To make the description about the proposed method understandable, Fig. 2 is taken as an example, which shows the system's hourly output from 19–25 December 2006 recorded in the database of the SCADA system.

Fig. 2 shows the variational features of the power output of PV system in sunny weather. From Fig. 2, it is found that the power output curves of PV system are similar in shape. Through the statistics and analysis of the database of the historical power data, if there is no change in day type, the output power on the forecasting day varies with the historical power output. Therefore in the forecasting model of the output power, the past relevant power output data are treated as input variable. Considering the number of the input variable, the forecasting model takes only the data of the day before the forecast day.

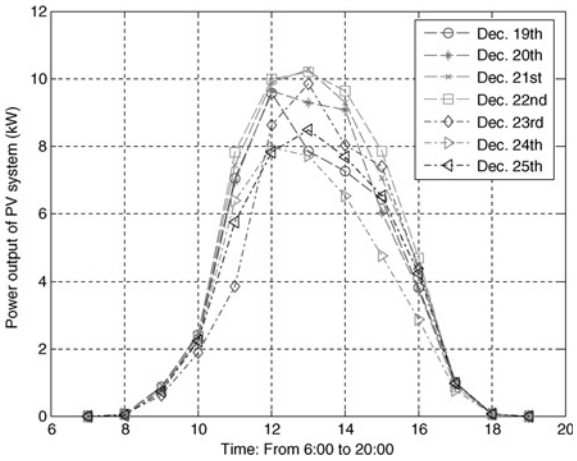

Fig. 2 *Power output of PV system in sunny weather*

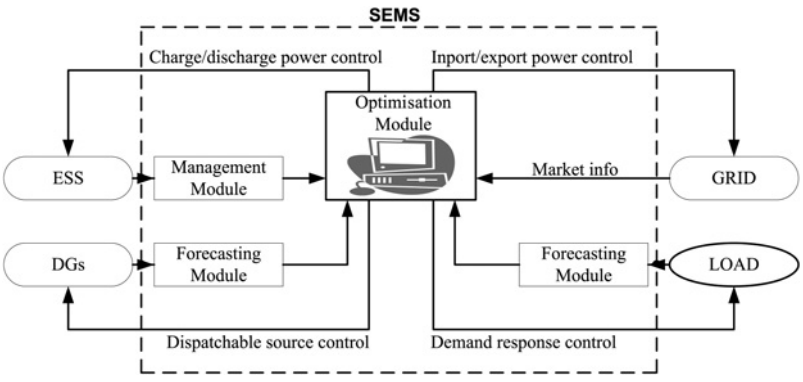

Fig. 1 *Schematic of the inputs and outputs of SEMS*

From Fig. 3, one can see that when it is sunny, the variation of power output of the PV system within 1 day can roughly reflect the variation of the solar irradiation intensity. However, when the day-type changes, from sunny to rainy, the power output will drop sharply. Without the input variable to reflect the change in solar radiation intensity, the prediction of the power output will become inaccurate. Therefore a proper variable should be chosen to show the drastic changes in the PV array power output when such changes occur. At present, with the constant improvement in the ability to forecast weather and network information, in establishing the forecasting model, if weather forecast information on forecasting day can also serve as one of the input variables, then the ability to forecast will improve. However, the meteorological parameters in weather forecast are usually described in the relatively ambiguous terms: for instance, sunny, sunny to cloudy, overcast, overcast with light rain, light rain to heavy rain etc. Thus, the conversion of ambiguous, uncertain and vague day type into the accuracy value, which can be accepted by the algorithm of the NN, requires enormous and effective power output for statistics and analysis. The paper expects to quantise the day type in light of the progressively perfect PV supervising system database.

Figs. 4 and 5 illustrate the PV array output power for cloudy and rainy days, respectively. The figures also show that the output power from 11 to 12 in the cloudy day is 2.666 kWh, and that (power output) from 11 to 12 in the rainy day is 0.367 kWh, whereas that (power output) from 11 to 12 in the sunny day is generally 9 kWh. Hence, based on the statistics of the historical power output data, such information as sunny, cloudy, rainy, overcast can be mapped as a day-type coefficient ranging from 0 to 1 and treated as the input variables of the forecasting model.

In addition to the historical output power and the day type discussed above, the effect of the air temperature on PV array power output should also be considered that historical output power data maps the shape of its curve, day-type information illustrates the rough height of the curve, and the air temperature in the same day type will show the delicate change of the curve's height, that is, the maximum power output. Figs. 6 and 7 show the daily output power of a PV array from 19 December 2006 to 26 December 2006 (the day type is roughly sunny) and the maximum air temperature in Wuhan urban area, respectively. The two charts demonstrate that higher power output of the PV system correlates to higher solar intensity, while under this condition the temperature is usually higher.

Meanwhile, seasonal factors also have effect on PV power output. Such an effect comes from the differences in solar radiation intensity; namely, the curve of the power output

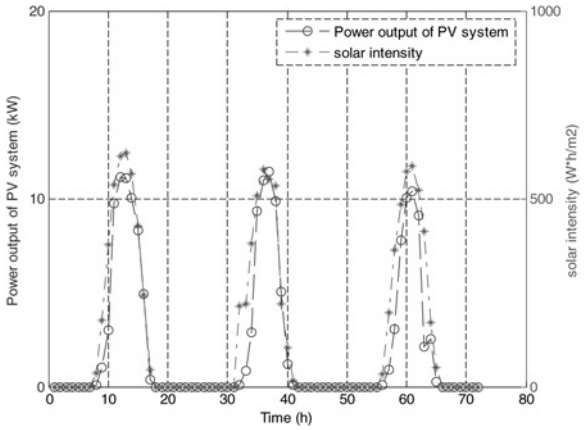

Fig. 3 *Power output of PV system and solar intensity in sunny weather*

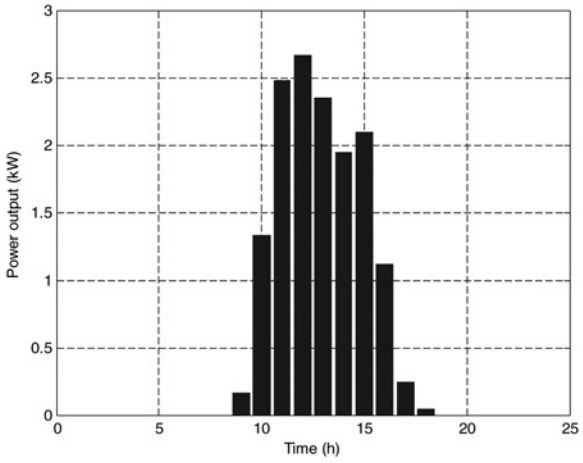

Fig. 4 *Power output of cloudy day*

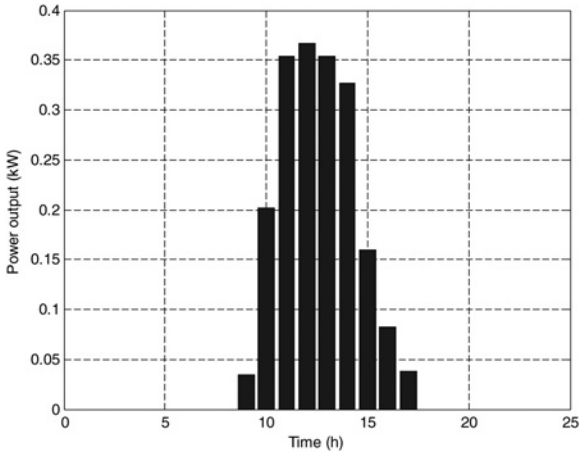

Fig. 5 *Power output of rainy day*

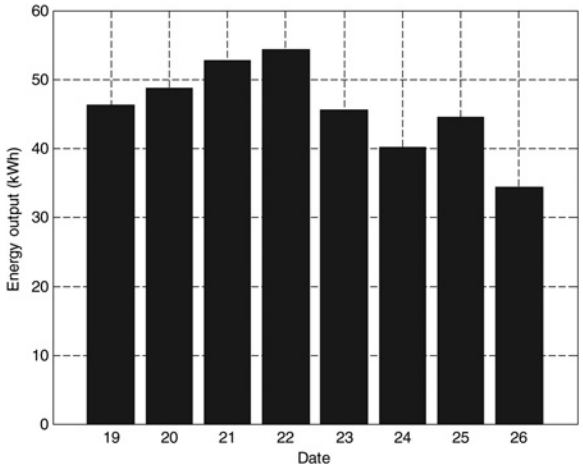

Fig. 6 *Daily overall energy output*

doi: 10.1049/iet-rpg.2010.0052

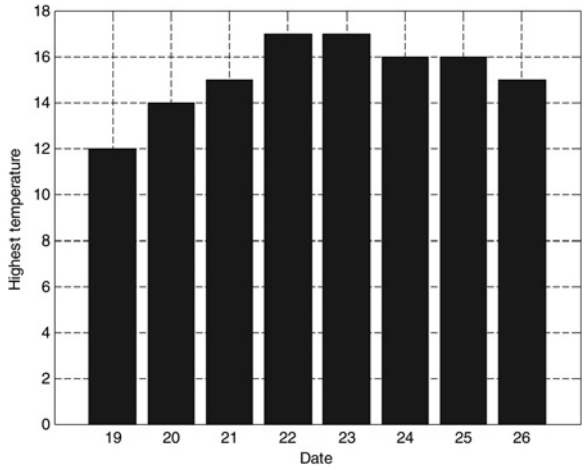

Fig. 7 *Highest temperature of several days*

changes with radiation intensity, seasonal differences in power output is also specifically illustrated. Moreover, due to the different geographical locations and the considerably different climates, the degree to which the effect of the seasonal factors on power output feature is also different.

The forecasting model is shown as Fig. 8, the input vector is $\boldsymbol{X} = (x_1, x_2, \ldots, x_{28})$, where $x_1, x_2, \ldots, x_{24}$ represent the generated energy of 24 time series of yesterday. $\boldsymbol{X}_{25}$ and x_{26} represent the highest temperature and day type of yesterday, $\boldsymbol{X}_{27}$ and x_{28} represent the highest temperature and day type of the forecasting day, respectively. Output variable y_1, $y_2, \ldots, y_{24}$ represent the forecasting generated energy of 24 time series of that day.

2.2 ESS management module

In practice, the ESS used in microgrid system consists of a matrix of identical batteries based on the size of PV power. Dozens of batteries would be connected in series to boost the voltage level of the battery matrix, whereas multiple battery strings are connected in parallel to increase the working current level of the battery storage system. We consider an aggregated ESS for representing batteries in a battery storage matrix.

The economics of the ESS are particularly complex, both because they require optimisation across multiple-time steps and because of the influence of tariff structures. Note that facilities with on-site generation will incur electricity bills more biased towards demand (peak power) charges and less towards energy charges, thereby making the timing and control of chargeable peaks of particular operational importance. Thus, the energy stored in the ESS are used as the state variable, the power output of the ESS can be calculated as the difference between stored energies of three

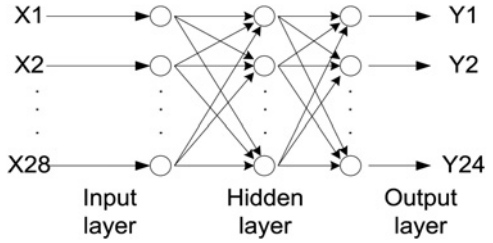

Fig. 8 *Topology of the forecasting module*

consecutive stages. Time stages used are all of 1 h. Energy stored in the storage device is expressed as follows.

1. If the ESS is charging ($P(t) < 0$)

$$-\eta_C P(t) \le K_C Q_s^{\max} \tag{1}$$

$$Q_S(t+1) = Q_S(t) - \eta_C P(t)\Delta t \tag{2}$$

2. If the ESS is discharging ($P(t) > 0$)

$$P(t)/\eta_D \le K_D Q_s^{\max} \tag{3}$$

$$Q_S(t+1) = Q_S(t) - P(t)\Delta t/\eta_D \tag{4}$$

3. If the ESS is idle ($P(t) = 0$)

$$Q_S(t+1) = Q_S(t) - W_{\text{hourly}} \tag{5}$$

where η_C is the charging efficiency, η_D is the discharging efficiency, K_C is the maximum portion of rated capacity that can be added to storage in an hour, K_D is the maximum portion of rated capacity that can be withdraw from storage in an hour, $Q_{\max}$ is the rated maximum stored energy, W_{hourly} (kWh) is ESS hourly discharged energy, $Q_S(t)$ (kWh) is aggregated capacity of all batteries at hour t, $P(t)$ (kW) is electrical power of ESS output at hour t and Δt is scheduling interval (1 h in this paper).

In order to establish an economical analysis, one must consider the ESS capital, operating and maintenance costs and parameters of which they depend, and energy purchase and sale costs.

ESS capital cost is defined as a function of two main parts. One is related to the storable energy; the other depends on the peak power that the storage must deliver and is controlled by the charge/discharge control system according to the demand requirements. Therefore the ESS capital cost will be expressed as

$$C_{\text{capital}} = C_P P^{\max} + C_W W^{\max} \tag{6}$$

where $P^{\max}$ (kW) and $W^{\max}$ (kWh) are ESS power and energy capacities, C_P (\$/kW) and C_W (\$/kWh) are their specific costs.

The hourly capital cost for ESS has been calculated from

$$C_1 = \left(\frac{r(1+r)^n}{(1+r)^n - 1}\right)\left(\frac{C_{\text{capital}}}{k * T_a}\right) \tag{7}$$

where r is the interest rate, n the depreciation period in years, C_1 is the hourly cost for depreciation, k is the capacity factor and T_a is their operating hours of the year.

Energy storage hourly operating and maintenance cost is defined as a function of two main parts: one related to the ESS rated power and the other depending on its hourly discharged energy

$$C_2 = C_O P^{\max} + C_M W_{\text{hourly}} \tag{8}$$

where C_O (\$/kW) and C_M (\$/kWh) are operating cost and maintenance costs.

Energy purchase cost is defined as

$$C_3 = \sum_{P(t)<0,t=1,\ldots,24} C_{\mathrm{T}}(t)P(t) \tag{9}$$

A total cost of all the considered costs is defined as

$$C_S = \sum_{i=1}^{3} C_i \tag{10}$$

In order to obtain the highest profit of energy prices differences between light-load and peak-load periods, energy storage charge/discharge operation must be scheduled such as, to store low-price energy during light-load periods and then to deliver it during peak-load ones. As a result of this strategy, load will be levelled according to time-of-use rates. The daily benefit because of this operation can be expressed as

$$C_4 = \sum_{P(t)>0,t=1,\ldots,24} C_{\mathrm{T}}(t)P(t) \tag{11}$$

where $C_{\mathrm{T}}(t)$ ($/kWh) is time-of-use rate in hour t, benefits can be made only if ESS efficiency is greater than the ratio (off-peak energy price/peak energy price).

The main goal of the ESS management module is to maximise the net present value. This net present value is determined through an economical analysis, over ESS lifespan, considering the ESS capital, operating and maintenance costs and parameters of which they depend, and energy purchase and sale costs. Based on (1)–(10), we formulate the net present value as follows

$$T_B = \sum_{t=1,\ldots,24} C_4 - \sum_{t=1,\ldots,24} C_{\mathrm{s}} \tag{12}$$

State of charge limits

$$Q_{\mathrm{s}}^{\min} \le Q_{\mathrm{S}}(t) \le Q_{\mathrm{s}}^{\max} \tag{13}$$

$$Q_{\mathrm{S}}(0) = Q_{\mathrm{I}} \text{ initial state of charge} \tag{14}$$

$$Q_{\mathrm{S}}(T) = Q_{\mathrm{E}} \text{ final state of charge} \tag{15}$$

Output power limits

$$P_{\mathrm{sl}}(t) = \min(\eta_{\mathrm{D}}(Q_{\mathrm{S}}(t-1) - Q_{\mathrm{s}}^{\min}),\ \eta_{\mathrm{D}}K_{\mathrm{D}}Q_{\mathrm{s}}^{\max}) \quad \text{if } P(t) > 0 \tag{16}$$

$$P_{\mathrm{sl}}(t) = \max((Q_{\mathrm{s}}^{\max} - Q(t-1))/\eta_{\mathrm{C}},\ K_{\mathrm{C}}Q_{\mathrm{s}}^{\max}/\eta_{\mathrm{C}}) \quad \text{if } P(t) < 0 \tag{17}$$

The equality constraint of the ESS periodical behaviour

$$\begin{cases} Q_{\mathrm{S}}(0) = Q_{\mathrm{I}} = Q_{\mathrm{S}}(T) = Q_{\mathrm{E}} \\ \dfrac{1}{\eta_{\mathrm{D}}} \displaystyle\sum_{P(t)>0,t=1,\ldots,24} P(t) + \eta_{\mathrm{C}} \sum_{P(t)<0,t=1,\ldots,24} P(t) \\ \quad + \displaystyle\sum_{P(t)=0,t=1,\ldots,24} W_{\mathrm{hourly}} = 0 \end{cases} \tag{18}$$

where $Q_{\mathrm{s}}^{\min}$ (kWh) is the minimum capacity of ESS, $Q_{\mathrm{s}}^{\max}$ (kWh) is the maximum capacity of ESS and $P_{\mathrm{sl}}(t)$ is the power limit of ESS at hour t.

2.3 Operation policies

According to the output of the power forecasting, the goal of the SEMS is to optimise energy flows among generation, supply and points of use to minimise operating cost or maximise profit while satisfying generating unit and network constraints. The output of this module is a set of recommended energy flows for a given period as a set of vectors from source to destination over each hour. The system can use available storage unit to offset expensive energy purchases or to store energy for an anticipated price spike. The optimisation procedure depends on the market policy adopted in the microgrid operation. In the following section, three possible operation policies are described.

1. The microgrid is separated from the upstream distribution grid and the SEMS aims to serve the total demand of the microgrid, using its local production. During the operating conditions, the SEMS minimises the operational cost of the microgrid, taking into account the regulation space of ESS, demand and DG bids. When the power produced by the local sources is greater than the load demand, if the remaining capacity of ESS is not enough, the excess power can be exported to the ESS; and if the remaining capacity of ESS is enough, the sources of high price can be closed to maintain the energy balance between supply and demand.
2. The SEMS aims at serving the total demand of the microgrid, using its local production, as much as possible, without exporting power to the upstream distribution grid. For the overall distribution grid operation, such behaviour is beneficial, because at the time of peak demand, when energy prices in the open market are high, the microgrid relieves possible network congestion by partly or fully supplying its energy needs. From the consumers' point of view, the SEMS minimises the operational cost of the microgrid, taking into account open market prices, demand and DG bids. The consumers of the microgrid share the benefits of reduced operational costs.
3. The microgrid participates in the open market, buying and selling active and reactive power to the grid, probably via an aggregator or similar energy service provider. According to this policy, the SEMS tries to maximise the value of the microgrid, that is, maximise the corresponding revenues of the aggregator, by exchanging power with the grid. The consumers are charged for their power consumption according to the bids of the generators. The microgrid behaves as a single generator capable of relieving possible network congestions not only in the microgrid itself, but also by transferring energy to nearby feeders of the distribution network.

2.4 Objective function

According to the first policy, the SEMS aims to minimise the microgrid operational cost by using its local production. The objective function for each hour intervals can be written as

$$T_{\mathrm{C}} = \sum_{t=1}^{T} \left\{ \sum_{i=1}^{L} [u_i(t)P_{\mathrm{G}i}(t)B_{\mathrm{G}i}(t) + S_{\mathrm{G}i}|u_i(t) - u_i(t-1)|] + \sum_{j=1}^{M} u_j(t)P_{\mathrm{S}j}(t)B_{\mathrm{S}j}(t) \right\} \tag{19}$$

doi: 10.1049/iet-rpg.2010.0052

where L is total number of generators, M is total number of storages, T is total number of hours, $u_i(t)$ is the status of unit i at hour t, $P_{Gi}(t)$ is active power production of the ith generator at hour t, $P_{Sj}(t)$ is active power production of the jth storage at hour t, S_{Gi} is the start-up or shutdown cost, $B_{Gi}(t)$ is bid of the ith generator at hour t, $B_{Sj}(t)$ is bid of the jth storage at hour t.

In the second policy, the SEMS sells energy to the consumers of the microgrid from the local sources and the upstream network. If the power produced by the DG sources is not enough or too expensive to cover the local load, energy is bought from the upstream network and sold to the consumers or stored in the ESS. Consumers and ESS are assumed to be charged at open market prices. If the power purchased from the upstream network is too expensive, the SEMS sells energy to the consumers from the local sources and the ESS.

$$T_{\mathrm{D}} = \sum_{t=1}^{T}\left\{\sum_{i=1}^{L}[u_i(t)P_{\mathrm{G}i}(t)B_{\mathrm{G}i}(t) + S_{\mathrm{G}i}|u_i(t) - u_i(t-1)|] + \sum_{j=1}^{M} u_j(t)P_{\mathrm{S}j}(t)B_{\mathrm{S}j}(t) + P_{\mathrm{GRID}}(t)B_{\mathrm{GRID}}(t)\right\} \quad (20)$$

where $P_{\mathrm{GRID}}(t)$ is power bought or sold from/to the utility at hour t, $B_{\mathrm{GRID}}(t)$ is energy price of the utility at hour t.

Different from the second policy, the SEMS of the third policy sells the excess production to the upstream network at the market price from the DG sources and the ESS. The total cost associated with energy production, energy storage and energy exchanging needs to be minimised over all problem variables.

2.5 Constraints

Unit constraints in SEMS, including unit capacity, ramping rates, minimum up/down, crew, fuel, start-up, shut-down, emission of individual units and a group of units, and ac power transmission constraints, calculates the commitment of units for supplying the hourly load. The constraints for the problem are given by

1. System power balance

$$\sum_{i=1}^{L} P_{\mathrm{G}i} + \sum_{j=1}^{M} P_{\mathrm{S}j} = D_{\mathrm{L}} \quad \text{In the first policy} \quad (21)$$

$$\sum_{i=1}^{L} P_{\mathrm{G}i} + \sum_{j=1}^{M} P_{\mathrm{S}j} + P_{\mathrm{GRID}} = D_{\mathrm{L}} \quad \text{In the second and third policies} \quad (22)$$

2. Spinning reserve constraint

$$\sum_{i=1}^{N} u(t)P_i^{\max}(t) \geq D_{\mathrm{L}}(t) + R(t) \quad (23)$$

3. Unit generation output limits

$$P_i^{\min} \leq P_i \leq P_i^{\max} \quad (24)$$

where $P_i^{\min}$ is the minimum power production of unit i, $P_i^{\max}$ is the maximum power production of unit I and D_L is the load demand.

3 MRC-GA optimisation module

In this work, the MRC-GA is developed to solve optimisation through genetic operations and avoid coping with economic dispatch problem in each hour. In the following sections the implementation of different components of the proposed algorithm are presented.

3.1 Coding

The solution of generator commitment in the SEMS is represented by a real-valued matrix.

$$G_k = [\boldsymbol{X}_1, \boldsymbol{X}_2, \ldots, \boldsymbol{X}_t, \ldots, \boldsymbol{X}_T] = [R_1, R_2, \ldots, R_i, \ldots, R_N]^{\mathrm{T}} = \begin{bmatrix} C_{1,1} & C_{1,2} & \cdots & C_{1,t} & \cdots & C_{1,T} \\ C_{2,1} & C_{2,2} & \cdots & C_{2,t} & \cdots & C_{2,T} \\ \vdots & \vdots & \cdots & \vdots & \cdots & \vdots \\ C_{i,1} & C_{i,2} & \cdots & C_{i,t} & \cdots & C_{i,T} \\ \vdots & \vdots & \cdots & \vdots & \cdots & \vdots \\ C_{N,T} & C_{N,2} & \cdots & C_{N,t} & \cdots & C_{N,T} \end{bmatrix} \quad (25)$$

where G_k is the kth individual of genetic populations; $C_{i,t}$ is the ith row, tth column element of coding matrix, which is power production of the unit i at time t; $\boldsymbol{X}_t$ is the tth column vector of coding matrix, which is load distribution among the units at time t; R_i is the ith row vector of coding matrix, which is short-term scheduling of the unit i.

The states of power generation units depend on the specific values of the real-valued matrix elements.

$$u(t) = \begin{cases} 0, & C_{i,t} = 0 \\ 1, & C_{i,t} \neq 0 \end{cases} \quad (26)$$

3.2 Generation of the initial group

The properties of initial group have an important impact on the efficiency of the calculation and the results. To achieve global optimal solution, the column matrix vector of the initial group should be coded in sequence. For example, the initialisation process of $\boldsymbol{X}_{\mathrm{t}}$ is as follows:

1. Generate an array of the random number A_{rand}

$$A_{\mathrm{rand}} = [a_{r1}, a_{r2}, \ldots, a_{ri}, \ldots, a_{rN}] \quad (27)$$

2. Calculate the array of the percentage coefficient P_{perc} from A_{rand}

$$P_{\mathrm{perc}} = [p_{p1}, p_{p2}, \ldots, p_{pi}, \ldots, p_{pN}] \quad (28)$$

$$p_{pi} = a_{ri} / \sum_{i=1}^{N} a_{ri} \quad i = 1, 2, \ldots, N \quad (29)$$

3. Initialise $\boldsymbol{X}_t$ as following

$$X_t = [C_{1,t}, C_{2,t}, \ldots, C_{i,t}, \ldots, C_{N,t}] \tag{30}$$

$$C_{i,t} = p_{pi} D_{\mathrm{L}}(t) \quad i = 1, 2, \ldots, N \tag{31}$$

3.3 Individual adjustment method

1. Owing to the accuracy requirements of unit commitment problem, each element of the vector $\boldsymbol{X}_{\mathrm{t}}$ should keep finite number of digits after the decimal point. Here, three digits are preserved.
2. Each variable is limited to its lower/upper bounds. We adjust the elements value of column $\boldsymbol{X}_{\mathrm{t}}$ to satisfy unit generation output limits. The method is as follows

$$C^*_{i,t} = \begin{cases} P_i^{\max}, & C_{i,t} > P_i^{\max} \\ C_{i,t}, & P_i^{\min} < C_{i,t} < P_i^{\max} \\ P_i^{\min}, & \lambda P_i^{\min} < C_{i,t} < P_i^{\min} \\ 0, & \text{else} \end{cases} \tag{32}$$

where $C_{i,t}$ is the value before adjustment; $C^*_{i,t}$ is the adjusted value; λ is the constant between 0 and 1, and in this paper is taken to 0.6.
3. To satisfy the system spinning reserve constraints, we adjust the states of the units. If $\sum_{i=1}^{N} u(t) P_i^{\max}(t) < D_{\mathrm{L}}(t) + R(t)$, a new unit will be open and its power output is equal to the least value.
4. After the above three-step adjustments, the sum of all elements of the column $\boldsymbol{X}_t$ may not be equal to the total system load at time t, thus making load distribution adjustment. Specific adjustment approach is as follows.

If $\sum_{i=1}^{N} u(t) P_i(t) < D_{\mathrm{L}}(t)$, power output of the ESS will be increased to meet the system power balance; on the contrast, if $\sum_{i=1}^{N} u(t) P_i(t) > D_{\mathrm{L}}(t)$, power output of the ESS will be reduced. In the adjustments, power output of the ESS is limited to its lower/upper bounds.

3.4 Selection of fitness function

After the individual adjustment method, the ESS commitment schedule obtained through GA relaxation may be infeasible for the equality constraint of the periodical behaviour. In practice, heuristic methods could be chosen to find a feasible solution. We pick the ESS commitment and send it to fitness function to guarantee that the final solution is feasible. In order to speed up the algorithm convergence, fitness function is defined as the following form

$$f_{\mathrm{fit}} = A/(T_{\mathrm{D}} + \sum_{i=1}^{M} \delta P_{\mathrm{eqi}}) \tag{33}$$

$$P_{\mathrm{eqi}} = \left| \frac{1}{\eta_{\mathrm{D}}} \sum_{P(t)>0, t=1,\ldots,24} P(t) + \eta_{\mathrm{C}} \sum_{P(t)<0, t=1,\ldots,24} P(t) + \sum_{P(t)=0, t=1,\ldots,24} W_{\mathrm{hourly}} \right| \tag{34}$$

where P_{eqi} is the violation value of the equality constraint of the ESS i periodical behaviour; δ is the punishment coefficient; A is the positive constant to calculate the fitness function, and in this paper is taken to 1 000 000.

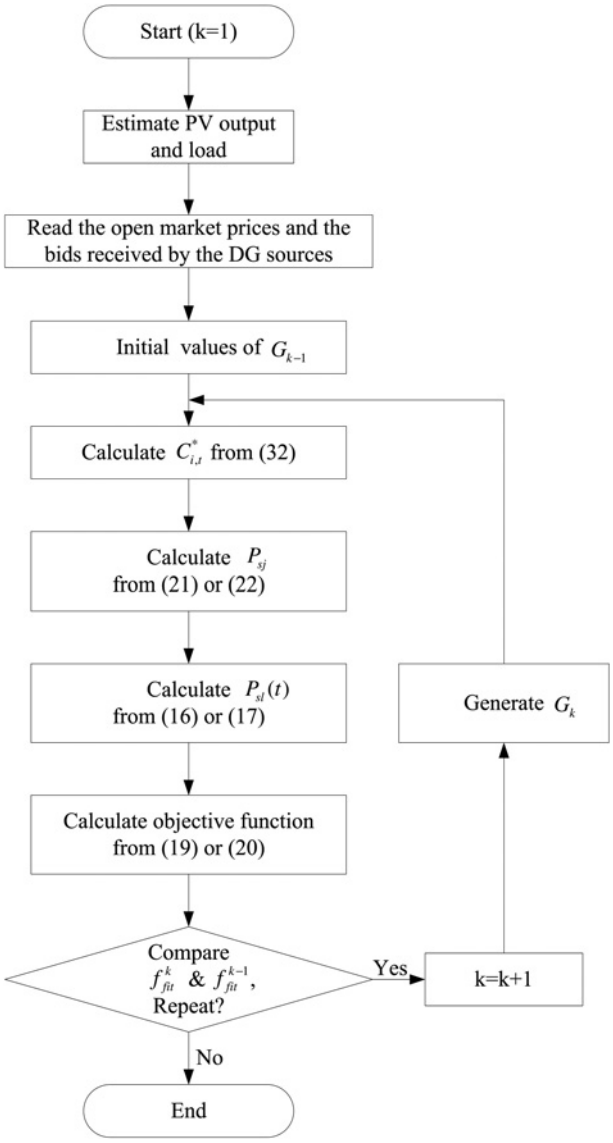

Fig. 9 *Iterative method*

According to the above-mentioned genetic algorithm, the optimisation problem is formulated and solved as a large-scale network problem with side constraints. Output from the model includes SEMS schedules, spinning and operating reserve, and trades curves such as that between fuel usage and the number of unit switches. The flowchart in Fig. 9 illustrates the implementation of this iterative technique.

4 Simulations and discussion

4.1 Power forecasting

Training data in the forecasting model were the historical generating data and meteorological data in the PV monitoring system. Two groups of data will be tested. In the first group, no day-type difference (three sunny days), in the second group, day type is different (the first two days are sunny and the third day is rainy).

Fig. 10 is the forecasting result, N1 is the forecasting net without the information of weather forecast, and N2 is the one with the weather forecast. It shows that when the day type is the same, the forecasting output of N1 has a similar

doi: 10.1049/iet-rpg.2010.0052

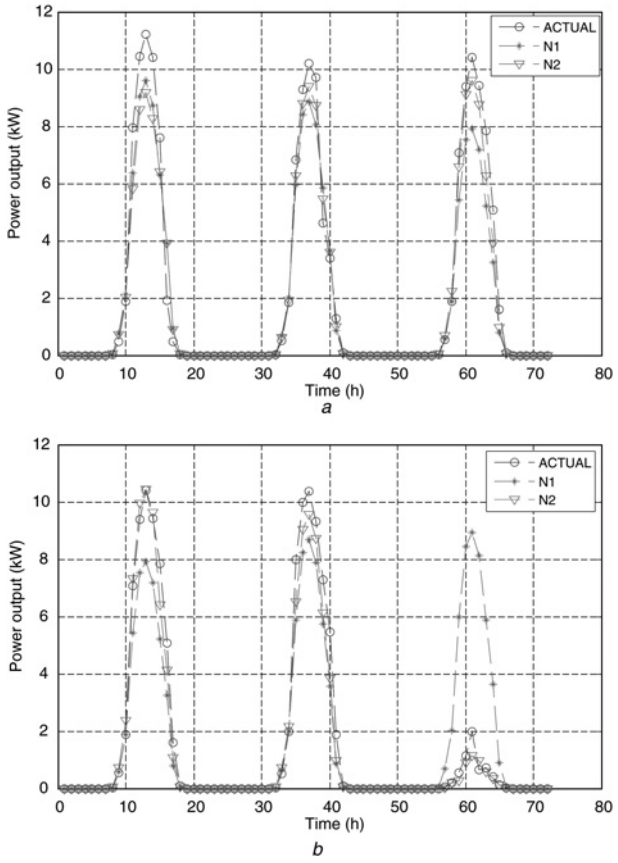

Fig. 10 *Forecasting results of the model*

a Day type is the same
b Day type is different

correspond to the actual power output as the N2 does, but slightly inferior in both accuracy and stability. However, when the day type is different, N1 failed, and N2 is effective with a decrease in the forecasting precision. Table 1 illustrates the mean absolute percent error (MAPE) of the forecasting model. When the day type is the same, the forecasting error of model N1 and model N2 is 16.47% and 11.59%, which was not big. However, when the day type is different, the error of model N 1 is 203.72%, which is a huge difference compared to the actual capacity, and this model failed. The forecasting error of model N2 is 18.91%, although there still exists difference compared to the actual figure, it still has high reference value.

Based on the effect analysis of day type, temperature and season on PV array power generation, neuron net was employed to design a new PV array power forecasting model. The historical data of the PV array were referred to in the forecasting model to forecast the generating capacity, reducing the influence on the forecasting precision because of the randomness of the PV cell and its installation set-up. At the same time, the information of the weather forecast was added to the input. When the day type is different, the forecasting model cannot fail.

Table 1 Mean absolute percent error

Number	Model N1, %	Model N2, %
(a)	16.47	11.59
(b)	203.72	18.91

4.2 Cost optimisation

In this study, the electricity sources include PVs, small wind turbines, microturbines, and fuel cells etc. The DG bids, the load bids, if demand-side bidding options are implemented, and the market prices are placed in one list according to their differential cost at the highest level of production for the specific period. This list is sorted in ascending order, until the total demand is met. The DG bids are assumed to be linear. Table 2 provides the minimum and the maximum operating limits of the DG sources. Table 3 summarises the bids coefficients assumed by the DG sources. Table 4 provides the load demand for local resident of the microgrid on a sunny day of December. Table 5 provides the hourly energy price of open market according to [7].

It is assumed that results obtained from the aforementioned analysis show that, without DG installations, the actual operating cost for the day considered is $303.9, and the price per kilowatt hour is $0.179. This is the base case scenario. Based on the power forecasting, SEMS provides the microgrid with an optimal schedule for each installed technology. The graphics in Fig. 11 show example SEMS operating results for the electrical balances of the microgrid on typical days. In these results, each with a slightly different optimal operation of the DG sources and it is

Table 2 Installed DG sources

ID	Type	Min power, kW	Max power, kW	Start up/down cost, $
1	MT	6	30	0.14
2	FC	3	30	0.24
3	FC2	2	20	0.18
4	PV	0	20	0
5	ESS	−33	30	0

Table 3 Bids of the DG sources

Hour	MT	FC1	FC2	PV
1	0.107	0.166	0.175	–
2	0.107	0.166	0.176	–
3	0.108	0.167	0.176	–
4	0.108	0.1677	0.177	–
5	0.109	0.167	0.178	–
6	0.109	0.168	0.179	–
7	0.11	0.168	0.18	–
8	0.111	0.169	0.181	0.084
9	0.112	0.170	0.183	0.085
10	0.112	0.171	0.186	0.086
11	0.116	0.172	0.187	0.087
12	0.117	0.171	0.188	0.088
13	0.115	0.170	0.187	0.086
14	0.115	0.170	0.186	0.085
15	0.115	0.170	0.187	0.084
16	0.117	0.171	0.187	0.083
17	0.118	0.173	0.189	0.085
18	0.119	0.173	0.190	0.086
19	0.118	0.174	0.191	–
20	0.115	0.173	0.189	–
21	0.112	0.171	0.186	–
22	0.110	0.170	0.185	–
23	0.109	0.169	0.183	–
24	0.108	0.167	0.182	–

Table 4 Typical load

t	1	2	3	4	5	6
P_L/kW	52	50	50	51	56	63
t	7	8	9	10	11	12
P_L/kW	70	75	76	80	78	74
t	13	14	15	16	17	18
P_L/kW	72	72	76	80	85	88
t	19	20	21	22	23	24
P_L/kW	90	87	78	71	65	56

Table 5 Hourly price of open market

t	1	2	3	4	5	6
$/kWh	0.033	0.027	0.020	0.017	0.017	0.029
t	7	8	9	10	11	12
$/kWh	0.033	0.054	0.215	0.572	0.572	0.572
t	13	14	15	16	17	18
$/kWh	0.215	0.572	0.286	0.279	0.086	0.059
t	19	20	21	22	23	24
$/kWh	0.050	0.061	0.181	0.077	0.043	0.037

presented in detail to demonstrate the scheduling capability. The various policies in the graphs indicate the different sources of the energy. The purple portion underneath the x-axis in these figures is the hourly storage charging of the ESS, whereas the portion above the x-axis indicates storage discharging. The blue portion of grid curve underneath the x-axis indicates the excess power of the microgrid that can be sold to the upstream distribution grid, whereas the other portion above it is the power purchased from the upstream distribution grid. In Table 6, the operational costs of the microgrid to run the computational simulations are considered.

As shown in Fig. 11*a*, the microgrid is separated from the upstream distribution grid and the SEMS aims at serving the total demand of the microgrid, using its local production. The SEMS sums up the DG sources bids in ascending order and the demand-side bids in descending order in order to decide which DG sources will operate for the next hour and which loads will be served. The daily costs are $286.69.

As shown in Fig. 11*b*, some generation capacity of the microgrid is replaced by storage and the upstream distribution, but the daily costs are reduced to ¥251.03. In other words, the added value of the storage and other complexity is very modest in this example. An explanation for this is that storage can take advantage of both economic and temporal inefficiencies, that is, by charging the battery via utility purchases during off-peak hours and then consuming the stored power during on-peak hours.

As shown in Fig. 11*c*, the SEMS sells energy to the consumers of the microgrid and also the excess production from the DG sources and the ESS, if any, to the upstream network at the market price. If the power produced by the DG sources is not enough or too expensive to cover the local load, power is bought from the upstream network and

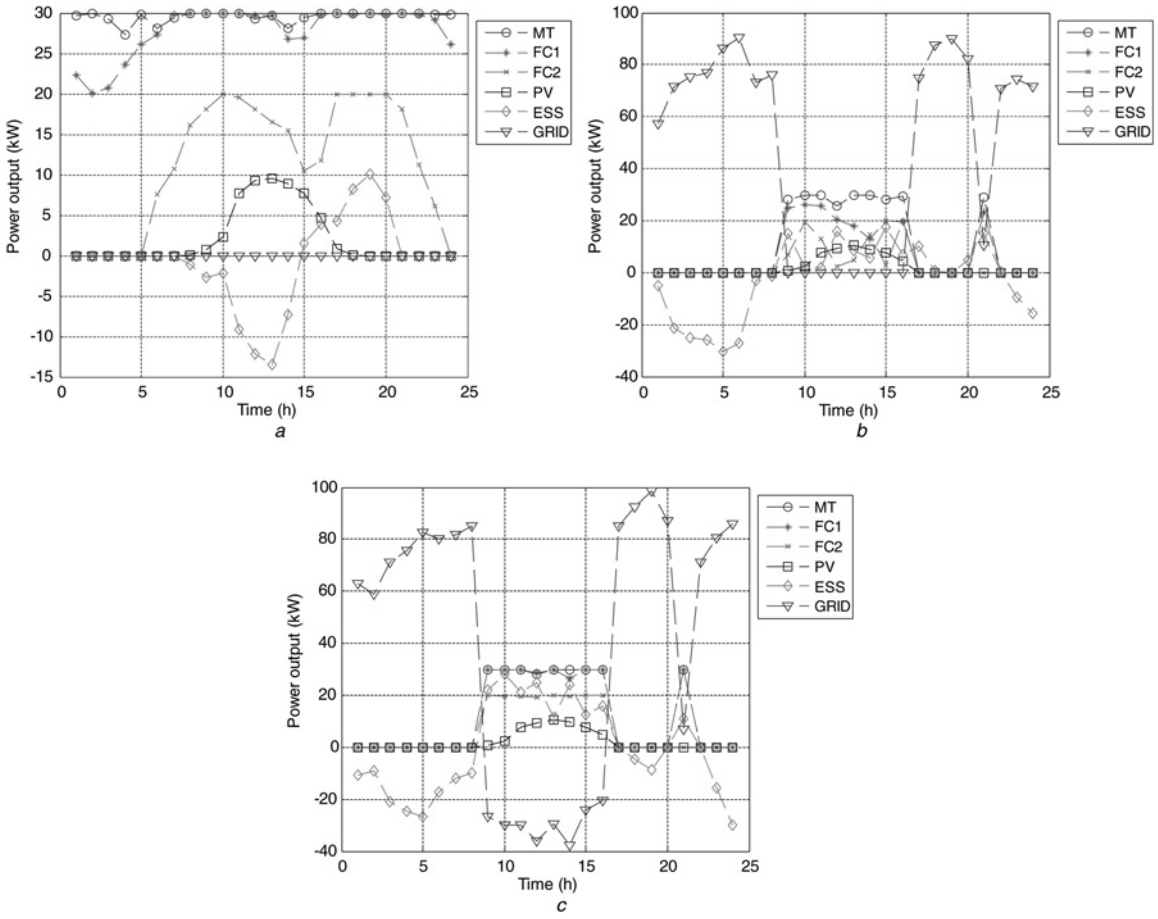

Fig. 11 *Typical operation results*

a Operation result in the first policy
b Operation result in the second policy
c Operation result in the third policy

doi: 10.1049/iet-rpg.2010.0052

Table 6 Economic savings using SEMS

Type	Costs	Savings
non-SEMS	303.9	–
policy 1	286.69	5.66%
policy 2	251.03	17.40%
policy 3	219.05	27.92%

sold to the consumers and the ESS. The daily costs are \$219.05, where the compensation to DG sources is \$262.15 and the profit of energy prices differences between light-load and peak-load periods is \$43.10.

5 Conclusion

In this paper, an SEMS has been proposed to optimally coordinate the power production of DG sources and ESS, and therefore minimise the operational costs of microgrids. The SEMS here takes an account of all relevant technical constraints, power forecasting, smart management of ESS, economic load dispatch and operational costs. The results show that the forecasting model is able to predict hourly power generation according to the weather forecasting inputs. Based on power forecasting, the SEMS is developed using MRC-GA optimisation module to make an optimal operation schedule in such way that economically optimised power dispatch can be maintained to fulfil certain load demand. It is also shown that, the SEMS is beneficial to reduce energy prices for the consumers and the daily costs are reduced by 27.92% below the third policy. Some further researches can be performed to perfect this method by concerning more relevant factors, such as the industrial and commercial profiles of a city or region. Diagrams corresponding to these factors will be done to reach more well-defined relationships between the optimal cooperation of the production of the DG sources and ESS and the operational costs of the microgrid.

6 Acknowledgment

The authors would like to thank the support from the National Natural Science Foundation of China under Project 50907027, the Special Fund for Meteorological Sciences Research in the Public Interest under Project GYHY201006036, and the National Basic Research Program (973 Program) of China under Project 2010CB227206.

7 References

1 Venkataramanan, G., Marnay, C.: 'A larger role for microgrids', *IEEE Power Energy Mag.*, 2008, **6**, (3), pp. 78–82
2 Marnay, C., Asano, H., Papathanassiou, S., Strbac, G.: 'Policymaking for microgrids', *IEEE Power Energy Mag.*, 2008, **6**, (3), pp. 66–77
3 Katiraei, F., Iravani, R., Hatziargyriou, N., Dimeas, A.: 'Microgrids management', *IEEE Power Energy Mag.*, 2008, **6**, (3), pp. 54–65
4 Sao, C.K., Lehn, P.W.: 'Control and power management of converter fed microgrids', *IEEE Trans. Power Syst.*, 2008, **23**, (3), pp. 1088–1098
5 Papadogiannis, K.A., Hatziargyriou, N.D.: 'Optimal allocation of primary reserve services in energy markets', *IEEE Trans. Power Syst.*, 2004, **19**, (1), pp. 652–659
6 Guerrero, J.M., Vasquez, J.C., Matas, J., Castilla, M., de Vicuna, L.G.: 'Control strategy for flexible microgrid based on parallel line-interactive UPS systems', *IEEE Trans. Ind. Electron.*, 2009, **56**, (3), pp. 726–736
7 Tsikalakis, A.G., Hatziargyriou, N.D.: 'Centralized control for optimizing microgrids operation', *IEEE Trans. Energy Convers.*, 2008, **23**, (1), pp. 241–248
8 Sortomme, E., El-Sharkawi, M.A.: 'Optimal power flow for a system of microgrids with controllable loads and battery storage'. 2009 IEEE/PES Power Systems Conf. and Exposition, 2009, pp. 1–5
9 Chakraborty, S., Weiss, M.D., Simoes, M.G.: 'Distributed intelligent energy management system for a single-phase high-frequency AC microgrid', *IEEE Trans. Ind. Electron.*, 2007, **54**, (1), pp. 97–109
10 Marnay, C., Venkataramanan, G., Stadler, M., Siddiqui, A.S., Firestone, R., Chandran, B.: 'Optimal technology selection and operation of commercial-building microgrids', *IEEE Trans. Power Syst.*, 2008, **23**, (3), pp. 975–982
11 Dukpa, A., Dugga, I., Venkatesh, B., Chang, L.: 'Optimal participation and risk mitigation of wind generators in an electricity market', *IET Renew. Power Gener.*, 2010, **4**, (2), pp. 165–175
12 Shafi, I., Ahmad, J., Shah, S.I., Kashif, F.M.: 'Evolutionary time-frequency distributions using Bayesian regularised neural network model', *IET Signal Process.*, 2007, **1**, (2), pp. 97–106
13 Pandey, S.N., Tapaswi, S., Srivastava, L.: 'Nodal congestion price estimation in spot power market using artificial neural network', *IET Gener. Transm. Distrib.*, 2008, **2**, (2), pp. 280–290
14 Amjady, N., Daraeepour, A., Keynia, F.: 'Day-ahead electricity price forecasting by modified relief algorithm and hybrid neural network', *IET Gener. Transm. Distrib.*, 2010, **4**, (3), pp. 432–444
15 Jewell, W.T., Unruh, T.D.: 'Limits on cloud-induced fluctuation in photovoltaic generation', *IEEE Trans. Energy Convers.*, 1990, **5**, (1), pp. 8–14
16 Rahman, Md.H., Yamashiro, S.: 'Novel distributed power generating system of PV-ECaSS using solar energy estimation', *IEEE Trans. Power Syst.*, 2007, **22**, (2), pp. 358–367
17 Kornelakis, A., Koutroulis, E.: 'Methodology for the design optimisation and the economic analysis of grid-connected photovoltaic systems', *IET Renew. Power Gener.*, 2009, **3**, (4), pp. 476–492